IOSR Journal of Electrical and Electronics Engineering (IOSR-JEEE)
e-ISSN: 2278-1676,p-ISSN: 2320-3331, Volume 19, Issue 1 Ser. 1 (Jan. – Feb. 2024), PP 38-44
www.iosrjournals.org

A study of a simulation perovskite-based solar cell HTM Layer IN PSCs

Dinesh Kumar Thakre[1], V. K. Suman[2]
1. Dinesh Kumar Thakre, PhD Scholer, Department of Physics, Malwanchal University, Indore, MP, India,
2. V. K. Suman, Professor, Department of Physics, Malwanchal University, Indore, MP, India

Abstract: Background: ***A*** *numerical analysis of an organohalide-based planar n-i-p perovskite solar cell (PSC) has been presented using the Solar Cell Capacitance Simulator (SCAPS-1D). The performance of the FTO/Ti02/perovskite/CZTS PSC structure has been investigated by varying the thickness of the absorber layer. The effect of the doping density of the absorber layer on PSC performance has been investigated using SCAPS simulation. Considering an absorber thickness of 220 nm and an absorber doping density of 10 15 cm3, the PSC performance is also investigated for various electron/hole transporting materials (ETMs/HTMs). It has been found that the properties of HTM affect PSC performance more significantly than those of ETM. Finally, it is observed that the CZTS-based PSC shows better performance than the CIGS-based PSC.*
Keywords: *PSC, Solar, HTM, PBS*

Date of Submission: 07-01-2024 Date of acceptance: 17-01-2024

I. Introduction:

The planar PSC commonly possesses a heterojunction architecture with three main layers, i.e., electron transport material (ETM), perovskite absorber, and hole transport material (HTM). The widely used ETM and HTM are TiO_2 and spiro-OMeTAD, respectively. Perovskite solar cells based on carbon electrodes (c-PSCs) without a hole transport material (HTM) have gained considerable interest owing to their cost-effective and simplified structure. However, their application is constrained by a combination of low efficiency and the prevalence of electron transport materials (ETMs), e.g., TiO2, which undergo extreme temperatures during their manufacturing processes. TiO2 also has poor optoelectronic properties, such as low conductivity and mobility. Additionally, when exposed to UV light, TiO2 susceptibility to photocatalysis reduces its long-term stability. In the present study, an HTM-free device based on FTO/TiO2/CH3NH3PbI3/carbon structure is employed and studied using a one-dimensional Solar Cell Capacitance Simulator (SCAPS-1D). Initially, the design is studied while employing inorganic ETMs.

Perovskite solar cells (PSC) are novel third-generation solar cells that use organometal halide perovskites as absorber material. There have been remarkable advances in the efficiency and performance of perovskite solar cells, from 3.8% in 2009 to 22.1% in 2017 [1]. The great advancement in perovskite solar cells was made possible by exploiting the high mobility, enhanced absorption coefficient, and tunable bandgap of the absorber material. Perovskite solar cells face major challenges like stability degradation, hysteresis, toxicity of lead, and the need for better encapsulation [2]. So there is an inevitable need to optimize the device parameters for reliable performance enhancement at a low fabrication cost.

The emergence of perovskite solar cells has attracted a lot of attention due to their high efficiency. However, the unstable performance and expensive hole transport materials limit its development [3]. Generally, organic materials (Spiro-OMETAD, PEDOT:PPS, MEH-PPV), which have relatively high cost and low hole mobility, are used as HTM in perovskite solar cells [4–5]. Some reports also showed that the HTM layer affects device performance, and the degradation of device performance was observed by using organic material as HTM [6–8]. Therefore, in order to commercialize perovskite solar cells and dominate the photovoltaic industry, it is necessary to find an alternative HTM layer for PSCs. Inorganic materials are considered promising materials for the HTM layer because of their favorable characteristics, such as high mobility of the hole, low cost of fabrication, better chemical stability, and appropriate valance band position [9–11]. Numerical simulation can be helpful in studying solar cell devices. SCAPS-1D has been developed by the University of Gent and has been widely used for thin-film solar cells. Perovskite solar cells with a planar structure have a similar structure and excitation type compared with thin-film solar cells. Therefore, many simulation-based PSCs have also been built using SCAPS. Hossain and co-workers built a simulation based on PSCs with ZnO as the ETM layer by using SCAPS. They showed that the device with ZnO as the ETM layer can obtain a high efficiency of 22.83% compared with TiO2 as the ETM layer [5]. The comparison of different organic hole

transport materials, including NPB, MEH-PPV, PEDOTPSS, Spiro-OMeTAD, and P3HT, was reported by Karimi and colleagues using SCAPS. They showed that the device with Spiro-OMeTAD as the HTM layer achieves the best performance [12]. A simulation of lead-free CH3NH3SnI3 perovskite solar cells was provided by Du and colleagues.

Device Model

The device model is built by SCAPS-1D software. The configuration of the perovskite solar cell used in this simulation is shown in Fig. 3.It is a planar heterojunction structure consisting of four layers. Following the direction of incident light, the device configurations are front contact (TCO), SnO2:F (FTO), n-type electron transportation layer (TiO2), perovskite material layer (CH3NH3PbI3), p-type hole transportation layer (Spiro-OMETAD,CuO,Cu2O), and back contact (Au).

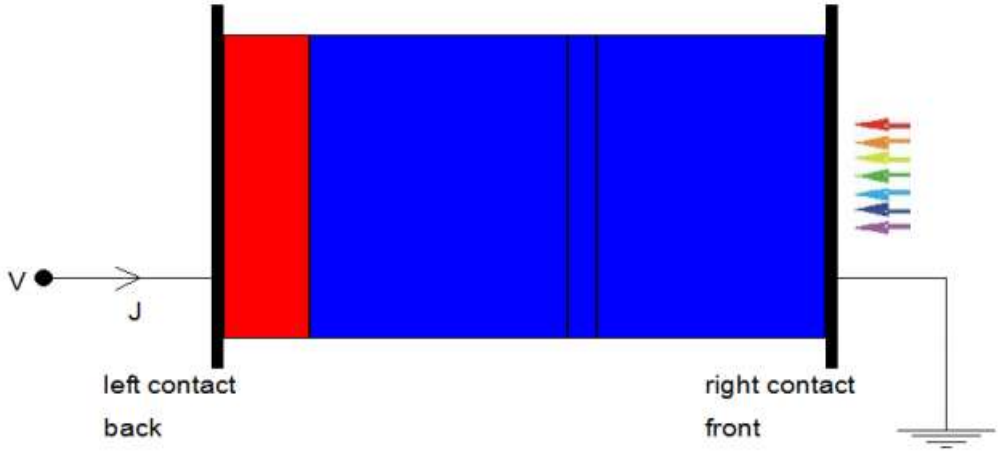

Fig.3.1.

The main idea of SCAPS-1D is to solve Poisson's equation and continuity equations for electrons andholes.

$$\frac{\partial^2}{\partial x^2}\varphi(x) = \frac{q}{\varepsilon}[n(x) - p(x) - N_D^+(x) + N_A^-(x) - p_t(x) + n_t(x)]$$

$$q\frac{\partial n}{\partial t} = \frac{\partial J_n}{\partial x} + qG - qR$$

$$q\frac{\partial p}{\partial t} = -\frac{\partial J_p}{\partial x} + qG - qR$$

$$J_n = qn\mu_n\frac{\partial \varphi}{\partial x} + qD_n\frac{\partial n}{\partial x}$$

$$J_p = -qp\mu_p\frac{\partial \varphi}{\partial x} + qD_p\frac{\partial p}{\partial x}$$

where φ is the potential, q is the elementary charge, Ɛ is the permittivity, n is the density of free electron, p is the density of free hole, N^+_D is the ionized donor-like doping density, N_A^- is the ionized acceptor-like doping density, p_t is the trapped hole density, n_t is the trapped electron density, G is the optical generation rate, R is the recombination rate, D_n is the electron diffusion coefficient, D_p is the hole diffusion coefficient, μ_n is the electron mobility, and $\mu_p$is the hole mobility. Here, it needs to set characteristics' parameters for each layer and device parameters in SCAPS. The parameters used in the simulation are adopted from literature, experimental work, and theoretical studies. The main parameters of materials and defects are summarized in Table 3.1(a) and Table 3.1(b) [13, 14–18]

Table 3.1(a): Materials parameters used in the numerical analysis

Parameters	FTO	TiO_2	$CH_3NH_3PbI_3$
Thickness(nm)	400	50	450
Acceptor density(cm^{-3})	0	0	0
Donor density(cm^{-3})	10^{19}	10^{17}	10^{13}
Bandgap energy(eV)	3.5	3.26	1.55
Electron affinity(eV)	4	4.2	3.9
Relative dielectric permittivity	9	10	6.5
Mobility of electron	20	20	2
Mobility of hole	10	10	2
Defect density(cm^{-3})	10^{15}	10^{15}	$2.5*10^{13}$

Other parameters of materials, such as the effective density of state of the conduction band and the effective density of state of the valance band, are set at 2.2×10^{18} cm3,while electron thermal velocity and hole thermal velocity are set at 1.8×10^{18} cm3, respectively. In order to simplify the device model, the absorption coefficient for each layer is set at 105 cm1, and the defect type is set at neutral, which means that the defect can lead to Shockley-Read-Hall recombination but cannot contribute to the space charge. The energetic distribution uses the Gaussian model, and its characteristic energy uses the default value.

The main device parameters are shown in Table 3.2. The standard AM1.5G spectrum is used in this simulation. The values of the working point and numerical setting use the default value. The scanning voltage is set from 0 V to 1.2 V. All the simulations will operate under these conditions.

Table 3.2: Device parameters used in the numerical analysis

Back contact electrical properties	
Thermionic emission/surface recombination velocity of electron(cm/s)	10^5
Thermionic emission/surface recombination velocity of hole(cm/s)	10^7
Metal(Au) work function(eV)	5.1
Front contact electrical properties	
Thermionic emission/surface recombination velocity of electron(cm/s)	10^7
Thermionic emission/surface recombination velocity of hole(cm/s)	10^5
Work function of TCO(eV)	4.4
Operation temperature(k)	300

II. Results And Discussion

The Influence of HTM Layer Characteristics

The investigation of the influence of HTM layer characteristics on device performance is based on Spiro-MeOTAD, which is widely used in current perovskite solar cells as a standard material. Hole mobility and

valance band gap offset are two crucial parameters that need to be considered as criteria in the selection of hole transport materials.

Hole mobility

The HTM layer without defects is applied here in order to see the effect of performance only caused by hole mobility.

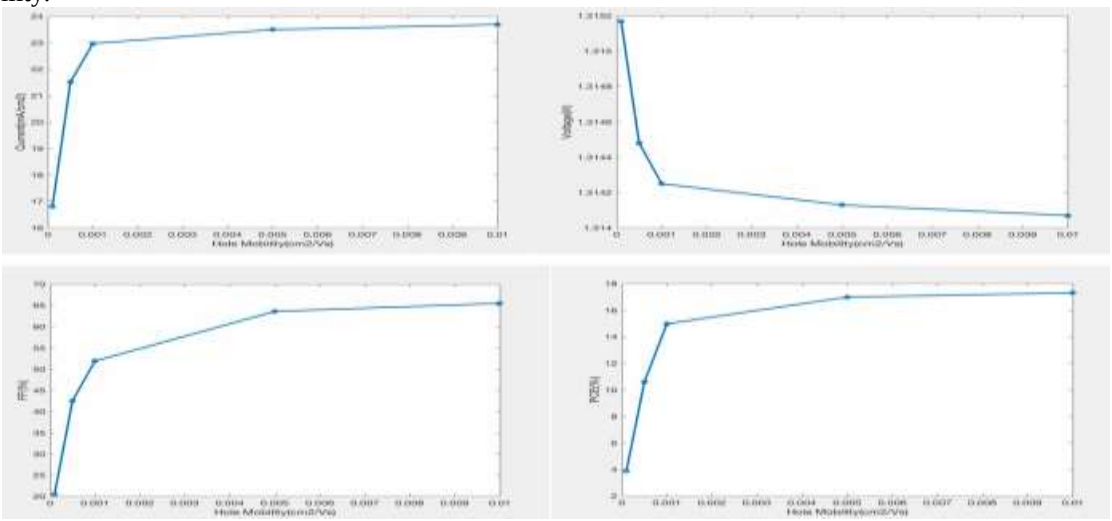

Fig. 3.2: The device performance for different hole mobility

Fig. 3.2 shows the simulation results by changing the value of hole mobility from 1e-4 cm2/Vs to 1e-2 cm2/Vs. The values of Isc, FF, and PCE gradually rise with the increase in hole mobility, while the value of Voc decreases slightly. Materials with large hole mobility should be considered for the selection of hole transport material.

Band gap offset

As we know, the HTM layer is used to transfer holes from the perovskite layer to the HTM layer while blocking the back charge flow from the HTM layer to the perovskite layer, so an appropriate valance band position is important in the device design. The influences of valance band offset on the device's performance are investigated in this section. The simulation results are shown in Figs. 3.3 and 3.4.

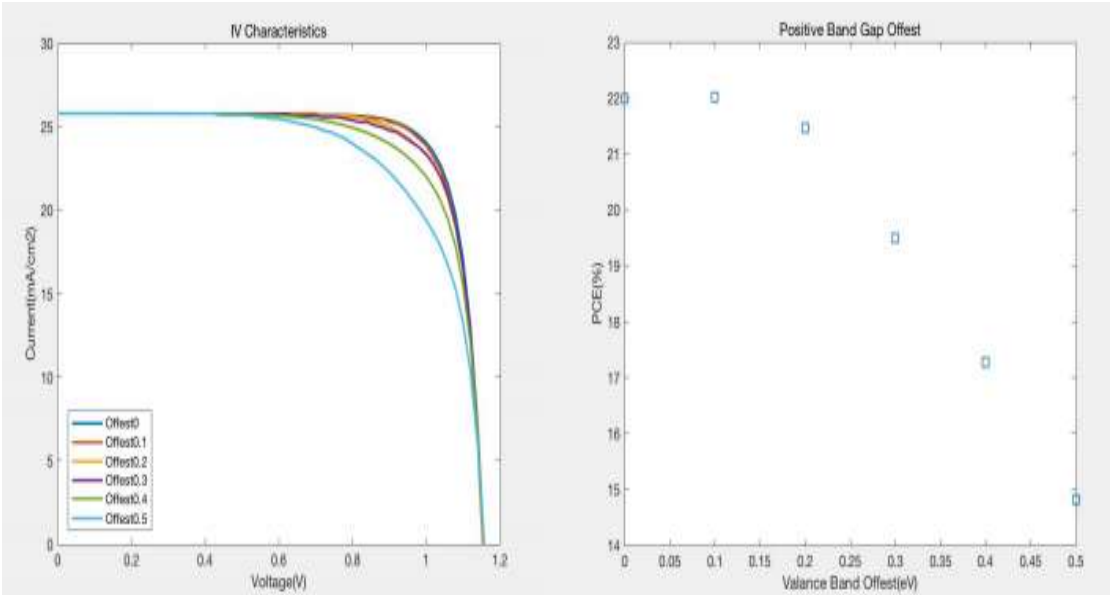

Fig. 3.3 shows the simulation results from different positive valance band gap offsets. In this case, the valance band position of the HTM layer is lower than that of the perovskite layer.

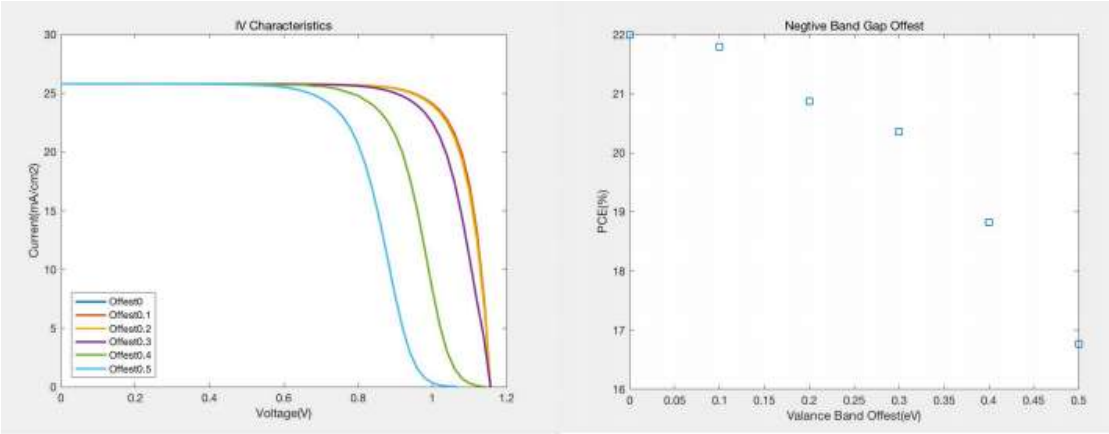

Fig. 3.4: Device performance for different values of negative valance band offset

Fig. 3.4 illustrates the simulation results from different negative valance band gap offsets. In this situation, the valance band position of the HTM layer is higher than that of the perovskite layer.

Comparison of Different Hole Transport Materials

Copper oxide (CuO) and copper oxide (Cu2O) are P-type semiconductors. Both of them have a relatively wide band gap. The band gap energy of CuO is 1.3 eV [18]. The band gap energy of Cu2O is 2.17 eV [19]. The energy level diagram of CuO and Cu2O in the device is shown in Fig. 3.5. From Chapter 3.3.1, In addition, Cu2O exhibits a high hole mobility of up to 80 cm2 V1 s1, and CuO also has a relative high hole mobility of 0.1 cm2 V1 V^{-1} s^{-1} compared with organic materials (Spiro-MeOTAD 0.0001 cm2 V1 V^{-1} s^{-1}). Therefore, for all these reasons that have been mentioned, it is believed that CuO and Cu2O are the probable alternative materials that can be utilized in HTM layers. The simulations are carried out by using three types of hole-transporting materials (CuO, Cu2O, and Spiro-MeOTAD).

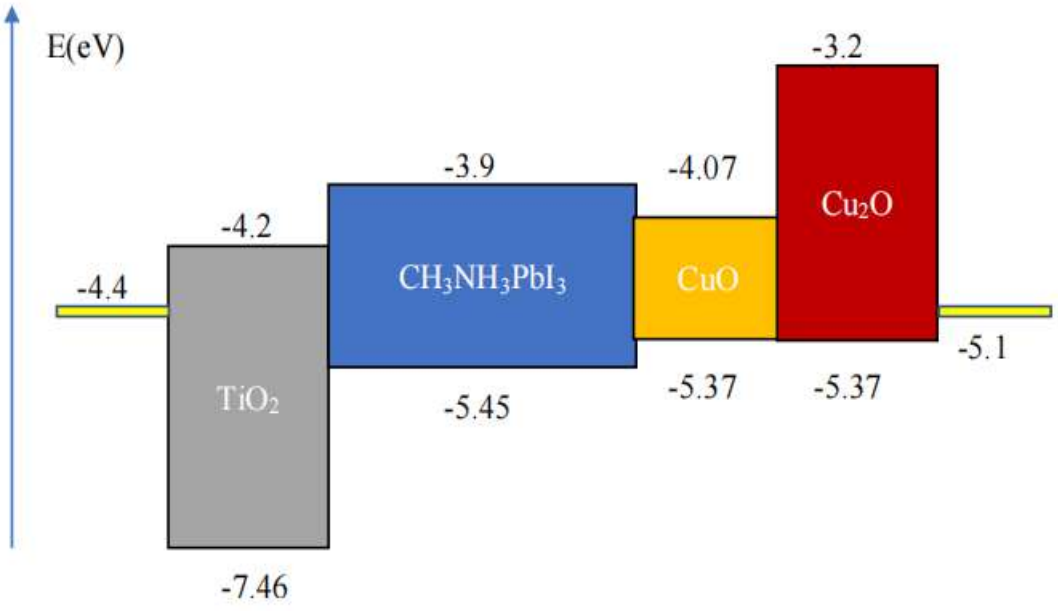

Fig. 3.5: Energy level diagram of CuO and Cu2O in the device

The simulation results are shown in Fig. 3.6 and Table 3.3. Fig. 3.6 illustrates the I-V characteristics of the perovskite solar cell with different HTM layers, including CuO, Cu2O, and Spiro-MeOTAD. Table 3.3 presents the results of device performance, including Isc, Voc, FF, and PCE for different HTM layers.

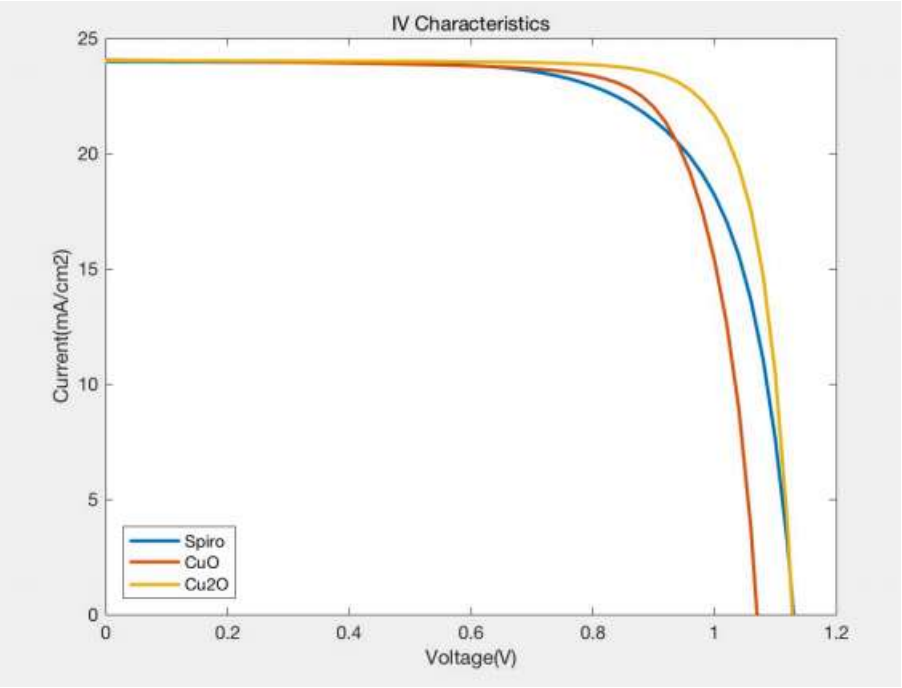

Fig. 3.6: I-V characteristics for different HTMs

Table 3.3: Device performance for different HTMs

HTMs	Isc mA/cm^3	Voc V	FF %	PCE %
Spiro-MeOTAD	23.93	1.13	71.24	19.32
CuO	24.04	1.07	77.05	19.83
Cu_2O	24.01	1.128	80.67	21.87

III. Conclusion

In this chapter, a device model with the structure ofglass/FTO/TiO2/CH3NH3PbI3/HTM/Au has been created using SCAPS-1D software. The effects of HTM layer characteristics, including hole mobility and valance band offset, have been discussed. The simulation results show that a high value of hole mobility in the HTM layer is good for device performance. For Spiro-MeOTAD, when hole mobility reaches 5e-3 cm2/Vs, PCE closes to the maximum value, and the change in it tends to become stable with the continuing increase of hole mobility.

References

[1]. World Energy Council, editor. World Energy Resources 2016 Survey.World Energy Council, 2016.
[2]. Shafiee, S., & Topal, E. (2009). When will fossil fuel reserves be diminished? Energy policy, 37(1), 181-189.
[3]. Qin, P., Tanaka, S., Ito, S., Tetreault, N., Manabe, K., Nishino, H., ... & Grätzel, M. (2014). Inorganic hole conductor-based lead halide perovskite solar cells with 12.4% conversion efficiency. Nature communications, 5, 3834.
[4]. Leng, C., Qin, H., Si, Y., & Zhao, Y. (2014). Theoretical prediction of the rate constants for exciton dissociation and charge recombination to a triplet state in pcpdtbt with different fullerene derivatives. The Journal of Physical Chemistry C, 118(4), 1843-1855.
[5]. Hossain, M. F., Faisal, M., & Okada, H. (2016, December). Device modeling and performance analysis of perovskite solar cells based on similarity with inorganic thin film solar cells structure. In Electrical, Computer & Telecommunication Engineering (ICECTE), International Conference on (pp. 1-4). IEEE.
[6]. Malinauska, T., Tomkute-Luksiene, D., Sens, R., et al., 2015. Enhancing thermal stability and lifetime of solid-state dyesensitized solar cells via molecular engineering of the hole transporting material spiro-OMeTAD. ACS Appl. Mater. Interfaces 7, 11107–11116.
[7]. Nguyen, W.H., Bailie, C.D., Unger, E.L., McGehee, M.D., 2014. Enhancing the hole- conductivity of spiro-OMeTAD without oxygen. J. Am. Chem. Soc. 136, 10996–11001.
[8]. Bailie, C.D., Unger, E.L., Zakeeruddin, et al, 2014. Melt-infiltration of spiro-OMeTAD and thermal instability of solid- state dye-sensitized solar cells. Phys. Chem. Chem. Phys. 16, 4864– 4870.
[9]. Li, M. H., Shen, P. S., Wang, et al. (2015). Inorganic p-type contact materials for perovskite-based solar cells. Journal of Materials Chemistry A, 3(17), 9011-9019.

[10]. Liu, L., Xi, Q., Gao, G., Yang, W., et al. (2016). Cu2Oparticles mediated growth of perovskite for high efficient hole-transporting-layer free solar cells in ambient conditions. Solar Energy Materials and Solar Cells, 157, 937-942.
[11]. Niu, G., Li, W., Meng, F., Wang, L., Dong, H., & Qiu, Y. (2014). Study on the stability of CH 3 NH 3 PbI 3 films and the effect of post-modification by aluminum oxide in all-solid- state hybrid solar cells. Journal of Materials Chemistry A, 2(3), 705-710.
[12]. Karimi, E., & Ghorashi, S. M. B. (2017). Investigation of the influence of different hole- transporting materials on the performance of perovskite solar cells. Optik-International Journal for Light and Electron Optics, 130, 650-658.
[13]. Tan, K., Lin, P., Wang, G., Liu, Y., Xu, Z., & Lin, Y. (2016). Controllable design of solid-state perovskite solar cells by SCAPS device simulation. Solid-State Electronics, 126, 75-80.
[14]. Casas, G. A., Cappelletti, M. A., Cédola, A. P., Soucase, B. M., & y Blancá, E. P. (2017). Analysis of the power conversion efficiency of perovskite solar cells with different materials as Hole-Transport Layer by numerical simulations. Superlattices and Microstructures, 107, 136-143.
[15]. Zhu L, Shao G, Luo JK. Numerical study of metal oxide heterojunction solar cells. Semiconductor Science and Technology. 2011 Jun 8;26(8):085026.
[16]. Goudarzi M, Banihashemi M. Simulation of an inverted perovskite solar cell with inorganic electron and hole transfer layers. Journal of Photonics for Energy. 2017 Apr;7(2):022001.
[17]. Minemoto T, Murata M. Impact of work function of back contact of perovskite solar cells without hole transport material analyzed by device simulation. Curr Appl Phys 2014;14:1428–33.
[18]. Sahdan MZ, Nurfazliana MF, Kamaruddin SA, Embong Z, Ahmad Z, Saim H. Fabrication and characterization of crystalline cupric oxide (CuO) films by simple immersion method. Procedia Manufacturing. 2015 Jan 1;2:379-84.
[19]. Scanlon, D.O., Morgan, B.J., Watson, G.W., 2009. Modelling the polaronic nature of p- type defects in Cu2O: the failure of GGA and GGA+U. J. Chem. Phys. 131, 124703.